Thermal Science and Engineering Progress 69 (2026) 104411

Contents lists available at ScienceDirect

Thermal Science and Engineering Progress

journal homepage: www.sciencedirect.com/journal/thermal-science-and-engineering-progress

Enhancing efficiency in Peltier-cooled atmospheric water harvesting: A mathematical modeling and experimental study☆

Parisa Heidarnejad [a,*], Egemen Sulukan [b], Abdullah Dedecan [b], Ali Kose [c], Furkan Yildirim [b]

[a] Yildiz Technical University, Mechanical Engineering Faculty, Department of Mechatronics Engineering, Istanbul 34349, Türkiye
[b] Istanbul Gedik University, Engineering Faculty, Department of Mechanical Engineering, Istanbul 34876, Türkiye
[c] Istanbul Gedik University, Gedik Vocational School, Istanbul 34913, Türkiye

ARTICLE INFO

Keywords:
Atmospheric water harvesting
Water scarcity
Peltier modules
Thermoelectric cooler

ABSTRACT

Water scarcity is one of the biggest global challenge, threatening current generation and necessitating alternative solutions. Among various technologies, atmospheric water harvesting systems offer a viable solution. The objective of this study is to present and assess an innovative geometry for Peltier-cooled atmospheric water harvesting system intended to improve drinkable water production through enhancing both mixing and heat transfer in the cold-side extended surfaces. The initial section of this study involves mathematical modeling. Findings of modeling section, illustrate an output of 1.97 L/day under conditions of 84.8% relative humidity and an ambient temperature of 32°C. The second section involves the design, fabrication, and performance evaluation of the system. The experimental observations indicate a water generation of 1.97 L/day in Test 1 (84.8% relative humidity, 32C), 1.63 L/day in Test 2 (85.8% relative humidity, 24.2C), 1.45 L/day in Test 3 (79% relative humidity, 25.4C), 1.29 L/day in Test 4 (76% relative humidity, 30C), and 1.13 L/day in Test 5 (69% relative humidity, 22.5C). These findings demonstrates the significant impact of environmental factors on the system's water generation performance. Moreover, novel geometry of the air inlet and exit channels improved the effectiveness of the water harvesting of the prototype across all test scenarios when compared with results reported in the literature. The outputs derived from modeling and experimental analysis, exhibit a strong correlation, thereby validating the model and highlighting the capability of the proposed system as a sustainable approach to global water scarcity problems.

1. Introduction

Access to clean and safe potable water continues to be one of the most critical global challenges of the 21st century. Based on the World Health Organization forecast, by 2025, approximately half of the world's population will live in regions enduring water stress [1]. Existing freshwater sources-such as rivers, lakes, and aquifers-are increasingly threatened by climate change, pollution, urban expansion, and unsustainable agricultural practices [2]. In response, researchers and engineers are actively investigating alternative water generation technologies that are sustainable, decentralized, and adaptable to diverse climatic conditions [3].

Among the emerging water generation technologies, Atmospheric Water Harvesting (AWH) has attracted considerable interest [4,5]. AWH systems are among the most innovative technologies that produce clean water by condensing moisture from the air. Although there is 14,000 km^3 of water in the atmosphere, considering that the amount of accessible water on Earth is only 1,200 km^3, the moisture in the atmospheric air can be seen as an inexhaustible water source [6]. AWH systems collect moisture in the atmosphere and condense it directly to form liquid water [7]. This approach is particularly promising due to the vast and continuously replenished atmospheric water reservoir. Furthermore, AWH systems can function independently of conventional water supplies, making them especially suitable for deployment in remote or off-grid regions where centralized water supply systems are unavailable or impractical [8–10].

AWH techniques mainly include absorption–regeneration, cooling air to dew point temperature [11] and, other technologies such as dew harvesting via passive radiative cooling [12,13]. Among these

☆ This article is part of a special issue entitled: 'Novel Thermal Applications' published in Thermal Science and Engineering Progress.

* Corresponding author.
E-mail address: parisa.heidarnejad@yildiz.edu.tr (P. Heidarnejad).

https://doi.org/10.1016/j.tsep.2025.104411
Received 1 October 2025; Received in revised form 28 November 2025; Accepted 6 December 2025
Available online 10 December 2025

Nomenclature

h_m	Mass transfer coefficient
D_h	Hydraulic diameter
R_v	Ideal gas constant
m_{water}	Condensable water mass flux
ΔT	Temperature difference
D	Diffusion coefficient
h	Heat transfer coefficient
I	Current (A)
k	Thermal Conductivity (W/(m.K))
N	Numbers of fins
P	Power (kW)
Q	Heat transfer rate (kW)
R	Thermal resistance (C/W)
Re	Reynolds number
RH	Relative humidity
S	Seebeck coefficient
T	Temperature (K), (C)
V	Voltage (V)
V	Water generation rate (m3/s)
α	Thermal diffusivity (m^2/s)
ρ	Density (kg/m3)

Subscripts

a	Ambient
c	Cold
dp	Dew point
h	Hot
m	Module
w	Water

Abbreviations

AWH	Atmospheric Water Harvesting
COP	Coefficient of Performance
PLA	Polylactic Acid
TEC	Thermoelectric Electric Cooler

techniques, cooling air to dew point temperature through thermo electric cooler (TEC) represents a solid-state active cooling technique that operates without generating noise or vibration, making it highly advantageous and particularly promising for localized cooling applications [14]. Additionally, TEC modules used in the AWH system are small and lightweight, enabling a simple installation with fewer system components and minimal maintenance requirements [15].

TEC modules or Peltier modules, based on Pletier effect consist of semiconductor thermoelectric element pairs (p-type, n-type) that operate on the thermoelectric cooling principle (Peltier effect). When direct current is passed through the module formed by these semiconductor pairs, heat is absorbed on one surface, creating a hot surface, while heat is emitted on the other surface, creating a cold surface [16]. It has been observed in the literature that cooling this hot surface with a fluid (water, air) significantly increases energy efficiency [17]. Single-stage Peltier coolers typically operate at a temperature difference of 23–30 °C, with the system's COP value reaching 0.5–0.7 [18]. Correspondingly, an electric current induces a temperature gradient across a semiconductor within Peltier modules. This gradient enables cooling on one side of the module, facilitating condensation as humid air passes over the cooled surface [19]. In the Peltier-based AWH system, heat exchange fins are located on the cold side and heat dissipation fins on the hot side to cool the cold surface of the Peltier module below the dew point temperature of the ambient air, causing water vapor in the air to condense on the surface and turn into liquid water. In AWH systems, fans are typically used to circulate humid air over the cold surface to increase condensation efficiency. Over time, innovative approaches have increased energy recovery, enabling greater water conversion [20].

Several researchers have assessed the performance of Peltier-cooled AWH systems. [21] evaluated the use of TEC to condense atmospheric moisture and produce freshwater. Results showed that energy consumption accounts for over 95 % of the water production cost and relative humidity strongly influenced saturation temperature, energy use, and overall productivity. [22] conducted experimental tests and numerical simulations for improving the efficiency of TEC-based AWH under controlled and real outdoor conditions. Numerical modelling showed temperature reduction along the airflow path due to condensation, and predicted water yield closely matched experimental results. [23] evaluated a combined adsorption–TEC to improve atmospheric water generation. They showed that hybrid case significantly yield higher water output compared to standalone TEC or adsorption units. The prototype produced 1.18 L/day with a generation cost of $0.33 per liter.

According to the literature, geometry of the prototype related to inlet and outlet air channels in Peltier-Cooled AWH systems has not been thoroughly investigated. The novel design of these channels with gradually expanding cross-sectional geometry facilitates the induction of air by the fans toward the cold-sided extended surfaces. This innovative geometry enhanced both mixing and heat transfer and improved the effectiveness in water harvesting. For this purpose, firstly a comprehensive theoretical model has been developed for the system. Subsequently, a prototype was developed in order to validate the model and operated in a laboratory-controlled environment. The experimental unit contains several Peltier modules, fans, aluminum fins, measurement devices and an external housing. Tests were performed through five scenarios with different air temperature and relative humidity values. Water generation rate and Coefficient of Performance (COP) as the primary performance indicators of the system were recorded and compared to the results of theoretical model.

2. Methodology

2.1. System description

Fig. 1 shows the working mechanism of the Peltier used in the Peltier-cooled AWH system. The ambient moist air is drawn into the channel by vacuum fans and directed over the cooling fins attached to the cold side of the Peltier modules. As the air passes through these fins, its temperature decreases below the dew point, leading to the initiation of the condensation process. Subsequently, the cooled and dehumidified air is directed over the fins attached to the hot side of the Peltier modules through cooling fans to facilitate heat dissipation. Finally, the air exits the channel after contributing to the thermal regulation of the system.

2.2. Mathematical modeling

This section addresses the mathematical modeling of the Peltier-cooled AWH system. Through employing concepts and equations that determine energy and mass transfer phenomena inside these systems, outcomes such as the COP and water production rate are assessed. Also the impact of different variables on their efficiency and water productivity is examined through this section. Since conducting experimental tests is both time-consuming and costly, mathematical modeling was performed as an effective approach for evaluating system performance under various environmental conditions, such as inlet air relative humidity and temperature enabling the identification of optimal operating

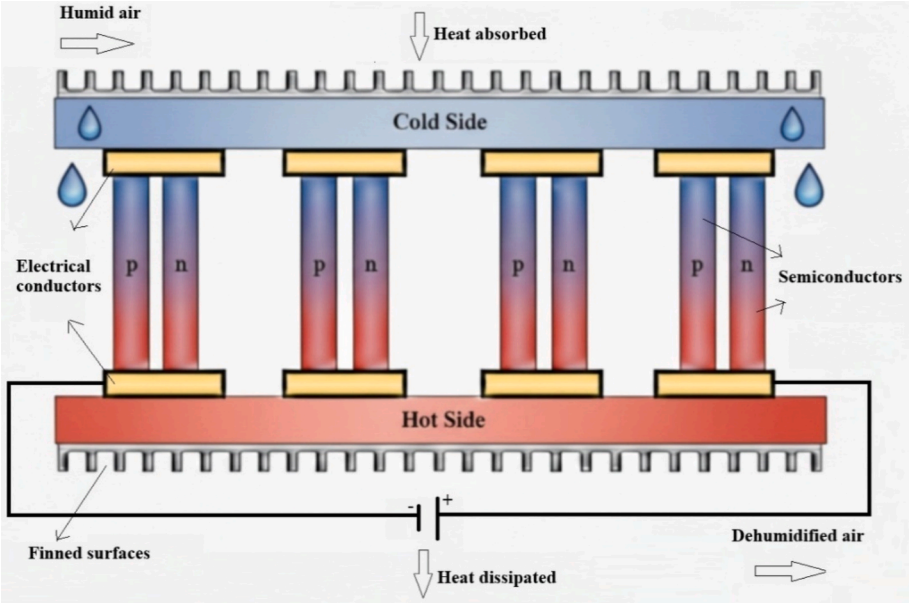

Fig. 1. Working principle of Peltier modules.

parameters. The governing equations related to each unit of the system are described in following subsections.

2.2.1. Peltier modules

A Peltier cooler module, also referred to as a Thermoelectric Cooler (TEC), utilizes two thin ceramic wafers with a series of p- and n-doped bismuth telluride (Bi_2Te_3) semiconductor materials positioned between them [24]. In the proposed Peltier-cooled AWH system, condensation of water vapor from humid air is facilitated through Peltier modules operating as a dehumidifier. Moisture-laden air passes to the extended surfaces connected to the cold side of the Peltier modules, where its temperature is dropped under dew point, resulting in condensation and the collection of potable water. Dehumidified chilled air flows over the extended surfaces connected to the hot side, with the aim of improving heat extraction from the hot side of the modules, therefore reducing their temperature and boosting the module's cooling efficiency. In this process, convection between air and extended surfaces, latent heat dissipation during condensation, and conduction through the Peltier modules are three pathways which result in heat transfer. Table 1 list the design parameters considered for the mathematical modeling of the Peltier modules.

The chosen Peltier model for the prototype is a commercially available module. TEC2-19006 from Int-El Electronics, utilizing Al_2O_3 as the thermoelectric material, including 190 couples, and supporting a maximum current of 6 A. Module's extensive availability, affordability, and minimal power use are three criteria for selecting it. Table 2 presents the performance characteristics of modules provided by the manufacturer.

The performance of the unit of Peltier modules can be evaluated through energy balance relations applied for the cold and hot sides. This analysis employs Fourier's law for heat conduction, convective heat transfer correlations, and latent heat calculations associated with condensation as outlined in the following. Accordingly, Q_C and Q_H are energy absorbed and dissipated from the cold side and hot side of a module respectively and can be calculated from below equations [25].

Table 1
Design parameters used for the mathematical modeling of the Peltier modules.

Parameter	Value
Ambient temperature (T_a)	32C
Voltage (V)	15 V
Hot side temperature (T_h)	27C
Temperature difference (TD)	7C
Number of Pletier modules	4

Table 2
Performance characteristics of TEC2-19006.

Dimensions (mm)	40x40	Maximum Voltage (V)	16
Maximum Power Consumption (W)	57	Maximum Current (A)	6
		Maximum Temperature of hot side (°C)	82

$$Q_c = S_m I T_c - \frac{I^2 R_m}{2} - k_m \Delta T \tag{1}$$

$$Q_h = S_m I T_h - \frac{I^2 R_m}{2} - k_m \Delta T \tag{2}$$

The terms S_m, R_m and k_m denotes the thermophysical properties of the module, namely Seebeck coefficient, thermal resistance and thermal conductivity. Parameter I represents electrical current, with T_h and T_c indicating the temperatures at the hot and cold junctions. Fundamental equations used to characterize Peltier modules involving the parameters I_{max}, V_{max}, ΔT_{max} and Q_{max} used are defined as follows (Z. [26].

$$S_m = \frac{V_{max}}{T_h} \tag{3}$$

$$R_m = \frac{(T_h - \Delta T_{max}) V_{max}}{T_h I_{max}} \tag{4}$$

$$k_m = \frac{(T_h - \Delta T_{max}) V_{max}}{2 T_h \Delta T_{max}} \tag{5}$$

The power consumption by modules (P_m) and COP can be computed as:

$$P_m = S_m I \Delta T + I^2 R_m \tag{6}$$

$$COP = \frac{Q_c}{P_m + P_f} \tag{7}$$

In which P_f denotes the total power consumed by the vacuum fans for

humid air intake and the cooling fans for maintaining adequate cooling of the hot side.

2.2.2. Condensing in cold-side extended surfaces

In order to approach condensation, the temperature of water vapor in the air must decrease to its saturation temperature [27]. For this reason, this study involved determining the dew point temperature and using temperature control to improve the energy required for water condensation. Dew point temperature is determined utilizing the renowned Magnus equation as below [28]:

$$T_{dp} = \sqrt[8]{\frac{RH}{100}}.(112 + 09.T_a) + 0.1.T_a - 112 \tag{8}$$

Where T_{dp} (℃) is the dew point temperature, RH (%) is relative humidity and T_a (℃) is the ambient temperature to be condensed, i.e. the air in the cold chamber.

The present study estimates the rate of water generation applying the one-dimensional conduction of Kiliç & Onat [29] formulated for condensation over fully wetted rectangular fins. The extended surfaces were designed with a base area of 0.49 m^2, same to the base area of the Peltier modules. Nineteen fins were chosen, each possessing a thickness of 1.3 mm. Aluminum ($k_f = 235$ W/(m·K)) is common fin materials, was utilized in this research. The operating parameters employed were T_∞ = 305 K, RH = 84.8%, and T_0 = 295 K. The experiments duplicated these circumstances for comparison. Also the following assumptions were made to simplify the analysis which are as follows Kiliç & Onat [29]:

- The fin tips are considered isolated;
- The variation of properties of air and water vapor is neglected along the fin;
- Processes take place under steady-state circumstances;
- Temperature of the fins are set to be below the dew point;
- The fin base and the cold side of the module are assumed to be in thermal equilibrium;
- The thermal conductivity of the fins and heat transfer coefficient are not varied;
- Pressure drop of the air flow is neglected;

Table 3 and Fig. 2 present the information related to the geometry of hot and cold-side extended surfaces which were used during the calculation of 1D heat conduction along the fins and the energy balance on the control volumes.

The condensable water mass flux (m_{water}) per unit of area in kg·m^{-2}·s^{-1} across the fin is determined using Equation 9, considering the latent heat of vaporization.

$$m_{water} = \frac{h_m}{R_v T_\infty}(P_{v,T_\infty} - P_{v,T}) \tag{9}$$

Establishing a correlation between heat and mass transmission was conducted utilizing Equation 10 [30]:

$$\frac{h_m}{h} = \frac{D}{k_{a,T_\infty}}\left(\frac{a_{a,T_\infty}}{D}\right)^{\frac{1}{3}} \tag{10}$$

Table 3
Geometry of cold and hot side extended surfaces.

	Cold side extended surfaces	Hot side extended surfaces
Number of fins	19	16
Shape of fins	Rectangular	Rectangular
Material of fins	Aluminum	Aluminum
Length of fins (mm)	35	49
Height of fins (mm)	180	220
Width of fins (mm)	1.3	3.5
Base area of extended surfaces (m^2)	0.49	0.385

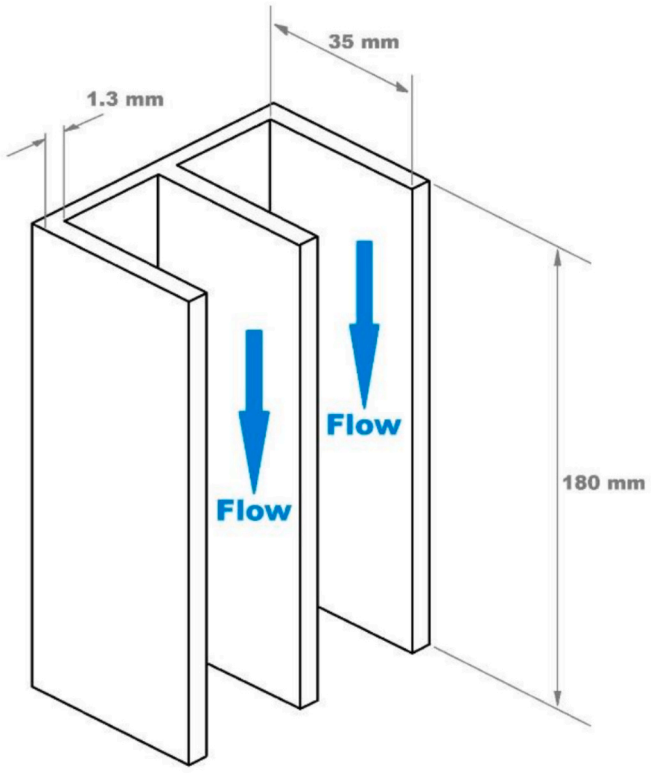

Fig. 2. Geometry of the cold-side extended surfaces.

$$D = \frac{2.2611x10^{-6}}{P_\infty}\left(\frac{T_f}{273}\right)^{1.81} \tag{11}$$

$$T_f = \frac{(T_r + T_\infty)}{2} \tag{12}$$

According to an experimental study by Coney et al. (1989), h can be estimated using Equation 13 which is valid for turbulent forced flow dehumidification over wet blunt-edge fins:

$$\frac{hD_h}{k_{a,T_\infty}} = 0.231\left|\frac{u_\infty D_h}{v_{a,T_\infty}}\right|^{0.69} \tag{13}$$

Reynolds number in the present study was calculated as 6919 which lies above the transitional range fully turbulent flow regime. Equation (13) was extracted for aspect ratio of approximately 16, representing a moderately thick geometry. In comparison, the fins used in this study have an aspect ratio of 26.9 corresponding to a somewhat slimmer geometry, yet both cases are within the same order of geometric slenderness. During the calculations, the fin-tip temperature was set below the dew-point temperature to guarantee that the entire fin surface remained in a fully wetted condition.

The rate of water production can be computed as given in Equation (14), where the factor of 2 accounts for condensation occurring on both surfaces of each fin:

$$V = \frac{2NbL_f m_{water}}{\rho_l} \tag{14}$$

2.3. System fabrication and experimental study

The geometry of the system housing was created and manufactured using SolidWorks, and 3D printer utilizing 1.75 mm PLA material. Firstly, ten separate parts were produced and then assembled to form the main body. The system incorporates four TEC2-19006 modules, which

were mounted onto the back on the extended surfaces with the aid of thermal paste. To minimize heat loss, cotton-based insulation pads were placed between hot and cold side extended surfaces. Additionally, the housing was covered with thermal insulation materials to enhance energy efficiency.

The AWH system operates with one vacuum fan to draw in the humid air which undergoes turbulent flow due to the gradually expanding geometry, slowing down beneath the cold side extended surfaces and facilitating dehumidification. The resulting dehumidified cold air is discharged at high speed and redirected over the hot side extended surfaces using an oval wall structure. This hot air is then drawn away by four cooling fans, ensuring effective cooling of the hot side, which is essential for the system's efficient operation. The condensed water is gathered at the oval base of the device.

A control panel to allow real-time monitoring of air temperature and relative humidity levels was considered. Additionally, the power supply feeding the Peltier modules can be adjusted via a dimmer, allowing voltage regulation with variation of ambient temperature and relative humidity, ensuring optimal operating conditions.

Fig. 3 illustrates the final prototype which consists of fans, aluminum fins, Peltier modules and measurement devices. Also, Fig. 4 shows a 3D design model of the prototype of the Peltier-cooled AWH system. The temperatures of all relevant temperature of cold-side and hot-side extended surfaces, air inlet and outlet, are measured using mini digital thermometers.The specifications of the measuring instruments are detailed in Table 4.

The novel geometry of the prototype related to inlet and exit air channels can be described as follows; the gradually expanding cross-sectional geometry facilitates the induction of air by the fans toward the cold-sided extended surfaces. When the airflow reaches the condensation zone, the oval-shaped side walls induce turbulence beneath the extended surfaces, enhancing mixing and heat transfer.

The incoming airflow is branched into two streams and begins to advance toward the cold-side extended surfaces. At approximately a 30° incidence angle, the first stream encounters the chamber, passes through the cold-side extended surfaces, and proceeds into the downstream chamber. The second stream moves forward in contact to the chamber and encounters the cold-side extended surfaces from the other side and this change in flow direction allows the air to stay in contact with the extended surfaces for a longer period, thereby improving the condensation capacity.

The discharge channel is specifically designed to slow down the air in order to prevent escaping. Dry air is slowed down up to ten times which happened by gradual narrowing. At the oval section of the discharge channel, the flow is divided into three streams. The right and left channels compress a portion of the air and direct it toward the oval wall on the outer perimeter, thereby preventing the cold air from mixing with the atmosphere. It enables the cooling fans to efficiently draw in cooled air, thereby enhancing overall cooling performance.

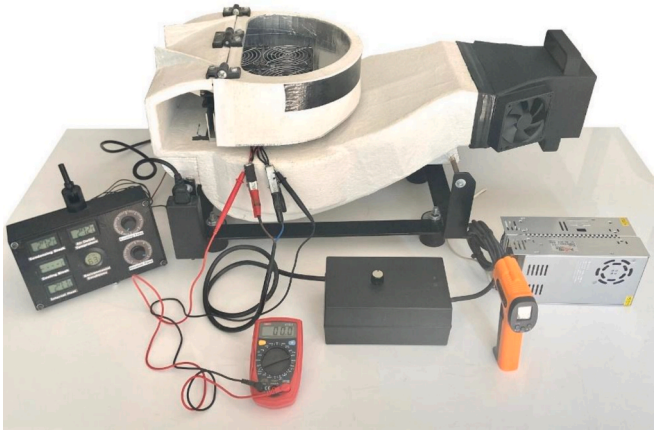

Fig. 3. Peltier-cooled AWH prototype.

This research examined five test scenarios with varying air temperature and relative humidity to assess water productivity and the COP of the system under different air conditions, as depicted in Fig. 5. The experiment was conducted over a duration of twenty-four hours to quantify the condensed water throughout this timeframe and to analyze the outputs. The maximum power delivered to the Peltiers modules considered to be around 139.6 W. Total power consumption of one vacuum fan and four cooling fans were 13.4 W which resulted in total power consumption of 153 W. The monitored outputs during tests incorporate inlet air temperature and humidity, average temperatures of the cold and hot-side extended surfaces, and the volume of condensed water collected.

2.3.1. Measurement uncertainty

This section analyzes uncertainties arising from instrument accuracy, operator errors, and parameter calculations. Primary parameters such as temperature, power input, and airflow carry uncertainties based on measurement device precision. Derived parameters, including COP, inherit uncertainty from variations in these primary quantities. The uncertainties of COP, input power, and cooling capacity are determined using their respective derivative-based formulations, as shown in Equations (14) and (15):

$$U_{COP} = \sqrt{\left(\frac{\partial COP}{\partial P}U_P\right)^2 + \left(\frac{\partial COP}{\partial Q}U_Q\right)^2} \tag{14}$$

$$U_{Q_c} = \sqrt{\left(\frac{\partial Q_c}{\partial T_c}U_{T_c}\right)^2 + \left(\frac{\partial Q_c}{\partial T_a}U_{T_a}\right)^2} \tag{15}$$

As listed in Table 5, the highest relative uncertainty between all parameters relates to Test 1, reaching roughly 4.89 %. Each test was replicated to verify the consistency of the measurements and experimental findings.

3. Results and discussion

The present section highlights the main findings related to the performance studies of the Peltier-cooled AWH system. It is categorized into two subsections: mathematical modeling and experimental work. The modeling part establishes a theoretical basis for estimating the influence of different key performance factors on water production rate and COP, while the experiments validate the model through data obtained from laboratory tests and delivers insights into the functional performance of the systems pursuant to several testing conditions.

3.1. Mathematical modelling of the Peltier-cooled AWH system

This section provides the outputs of the mathematical modelling of the Peltier-cooled AWH system analyzing the influence of fin length, ambient air temperature and ambient relative humidity on the water productivity and COP of the system.

3.1.1. Influence of fin length on daily water generation and COP

This study examines the influence of fins length of the fins on water productivity and COP under constant atmospheric conditions which is presented through Fig. 6. The material of the fins are selected to be Aluminum since it is cost effective, light and good thermal conductor. Findings show that the water production improves with fin length but at a diminishing rate until a maximum is attained. This result highlight that in the design of fins, both latent heat and mass transfer should be consiederd. The water generation rate is not assessed across the whole range of fin lengths, as longer fins may result in higher temperatures and the appearance of dry regions around the fin tips. In dry regions, where

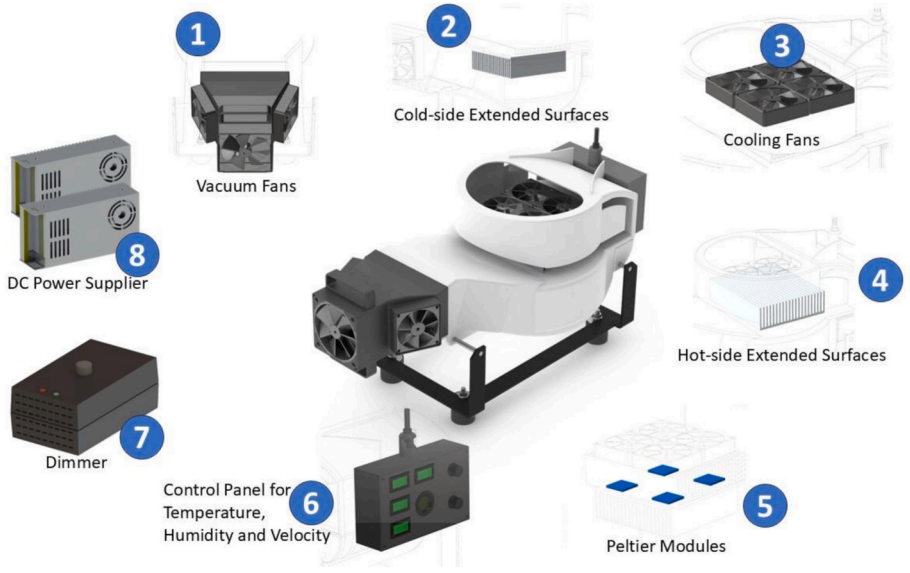

Fig. 4. 3D design model of the prototype of the Peltier-cooled AWH system.

Table 4
Details specifications of the measuring equipment used in experiments.

Instrument	Application	Accuracy/ Resolution	Photo
Mini Digital Thermometer	To measure the temperature of cold-side and hot-side extended surfaces, air inlet and outlet	±1°C/0.1°C	
Humidity meter	To measure environmental conditions e.g. humidity and temperature	±%5 RH/%1 RH	
Non-contact infrared temperature meter	To monitor the instant temperature of all surfaces	±1.5°C/0.1°C	
Digital multimeter	To measure the current and voltage of the system	±(1 % + 2 digit) (A) ±(1.2 % + 10 digit) (V)	

temperatures surpass the dew point, water condensation fails to occur, markedly diminishing water output due to the decreased effective surface area for phase change. Maximum water production takes place at a fin length of 0.048 m. However, beyond this peak point of water productivity, the COP starts to decline as the fins get longer. This is attributed to the fact that both electricity consumption and cooling capacity increase steadily with longer fin lengths; however, the rate of increase in electricity consumption surpasses that of the cooling capacity. The system reaches its maximum COP with a fin length of 0.025 m.

3.1.2. Influence of relative humidity on daily water generation and COP

Ambient relative humidity significantly influences the performance of water generating devices, especially those utilizing Peltier modules. Fig. 7 depicts the association between ambient relative humidity and daily water production in the Peltier-cooled AWH system, demonstrating a positive linear relationship. Higher relative humidity means higher concentration of water vapor in the surrounding air which results in greater condensation of water vapor, as this humid air passes the cold extended surfaces. The unit generates a maximum of 3.6 L of water daily when the air's relative humidity attains 96%. Conversely, low relative humidity indicates a reduced availability of water vapor for

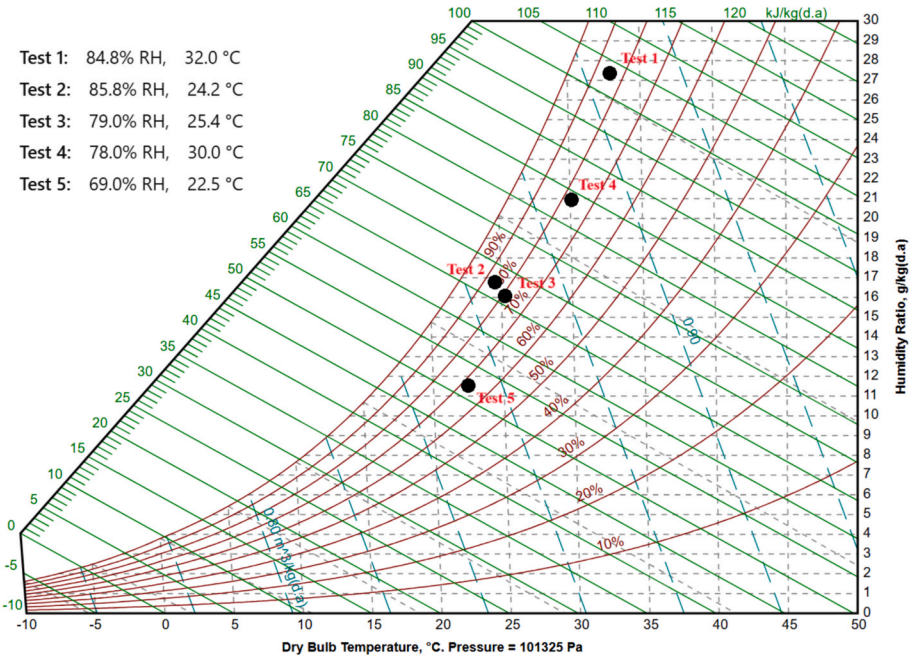

Fig. 5. Five different test scenarios and their corresponding locations on Psychrometric diagram.

Table 5
Relative uncertainties of COP for all five tests.

Test number	Value of calculated COP based on experiments	Relative uncertainty of COP
1	2.57	4.89%
2	1.23	2.56%
3	1.90	1.93%
4	1.78	2.38%
5	1.12	0.73%

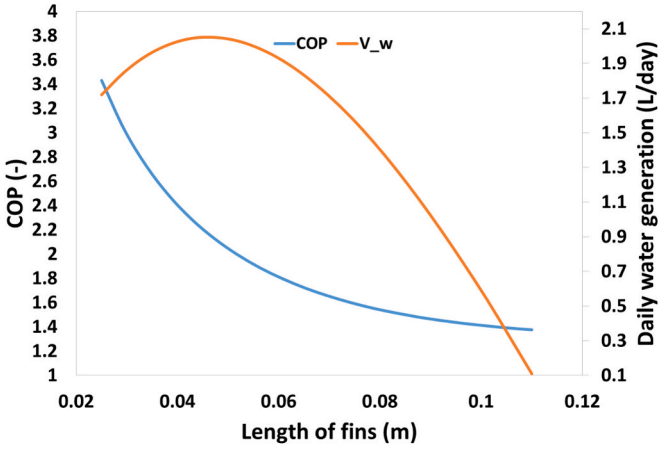

Fig. 6. Influence of fin length on daily water generation and COP of the Peltier-cooled AWH system.

condensation, leading to considerably lower water production. Although the cooling system may continue to efficiently lower temperatures, the water production rate will be negligible. An elevation in relative humidity improves water generation efficiency, as a greater concentration of water vapor in the atmosphere promotes condensation and decreases the energy necessary to cool the air to its dew point. This phenomenon clarifies the nearly doubling increase in COP as relative humidity escalates from 76% to 96%. On the other hand, low relative

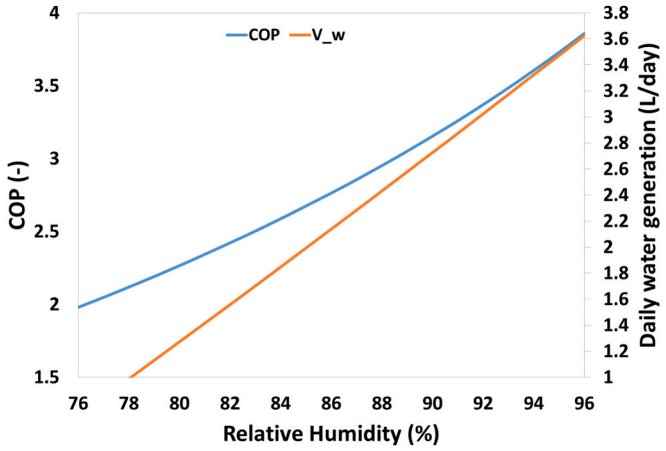

Fig. 7. Influence of air relative humidity on daily water generation and COP of the Peltier-cooled AWH system.

humidity leads to decreased water production and necessitates increased energy consumption, hence decreasing the water harvesting performance of the system.

3.1.3. *Influence of ambient temperature on daily water generation and COP*

The impact of air temperature besides relative humidity in determining the water production rate of Peltier-Cooled systems, making it crucial in optimizing AWH systems. Fig. 8 presents that, ambient temperature has a substantial impact on the water productivity in Peltier-cooled AWH systems. When the ambient air temperature increases between 26℃ and 34℃, the capacity of the air to retain water vapor rises, resulting in nearly 1.4 times more water available for condensation. The air maintains less moisture at lower temperatures, which makes it difficult to condense and extract water. In other words, in conditions of high relative humidity, higher temperatures result in higher levels of water vapor production, as warmer water can take in more water vapor. Moreover, high temperatures can also amplify the COP of the cooling system, since both Q_c and P_m in Equation 7 decreases but the slope of decrement of P_m is higher than Qc and as a result, COP rises by about

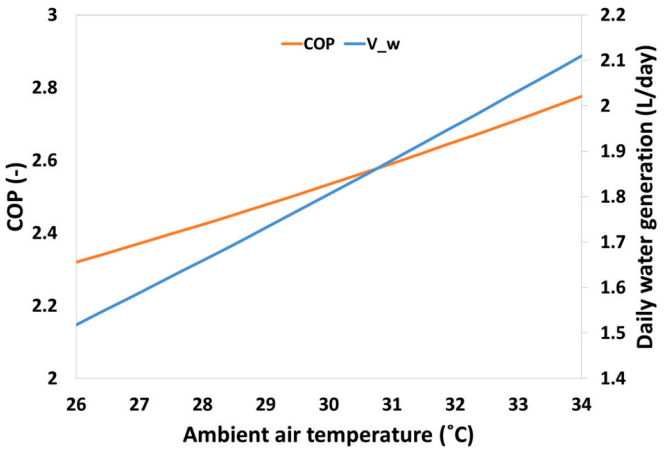

Fig. 8. Influence of ambient air temperature on daily water generation and COP of the Peltier-cooled AWH system.

Fig. 10. Condensing water on the cold-side extended surfaces.

52% as ambient air temperature increases from 26℃ to 34℃.

3.2. Experimental study of the Peltier-cooled AWH system

The experimental studies of the Peltier-cooled AWH system were carried out at the College of Engineering, Istanbul Gedik University, located at 40.90° N latitude and 29.22° E longitude, Istanbul, Türkiye. Fig. 9 illustrates the average monthly temperature and relative humidity data for the examined site. The experimental tests are carried out to verify the findings of the mathematical modeling. The main aim of these experiments is to examine the influence of ambient temperature and relative humidity on the water generation rate and COP. The experimental system mainly functions within a temperature range of 22℃ to 32℃ and a relative humidity range of 68% to 85% RH.

3.2.1. Comparison of mathematical modeling and experimental results

Mathematical modeling and experimental analyses of the Peltier-cooled AWH system were carried out under five different test conditions, as defined in Fig. 5. Fig. 10 clearly shows the formation of water droplets on the cold-side extended surfaces resulting from the condensation of ambient air cooled below dew point temperature during five mentioned test conditions. The daily water generation across all five test scenarios are presented in Fig. 11. As illustrated in Fig. 11, Test 1, Test 2,

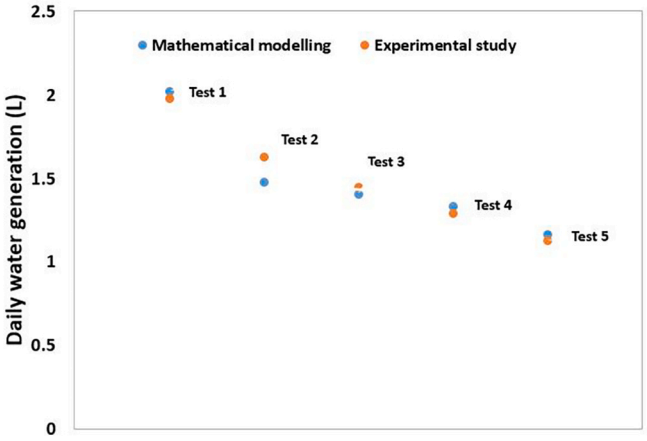

Fig. 11. Daily water generation for different five test conditions in the Peltier-cooled AWH system during mathematical modeling and experimental studies.

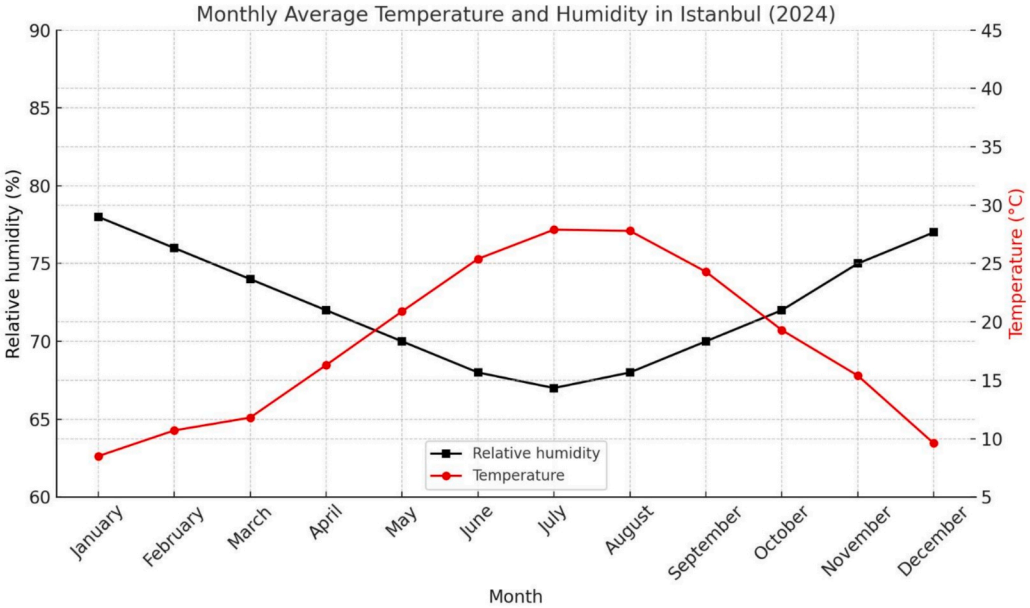

Fig. 9. Monthly variations in the average temperature and relative humidity of the region.

Test 3, Test 4, and Test 5 rank in descending order of performance based on the total amount of water harvested over a 24-hour period. Test 1, characterized by the highest ambient temperature, exhibited the maximum water generation, while Test 2, which featured the highest relative humidity, yielded the second-best performance. These results highlight the dominant influence of both temperature and relative humidity on water harvesting efficiency. An increase in temperature raises the absolute humidity of the air, thereby increasing the available water vapor for condensation. Consequently, Test 1, with the highest temperature, contained the greatest amount of water vapor among all tests, resulting in enhanced water collection. Likewise, Test 4 demonstrates the positive relationship between water generation rate and relative humidity.

Conversely, Test 5, which had the lowest temperature and relative humidity, showed the poorest performance in terms of water generation. Furthermore, Fig. 11 presents a comparison between the results of the mathematical model and experimental measurements across all five test scenarios. A strong agreement is observed between the two, confirming the validity of the model. In both simulation and experiment, the Peltier-cooled AWH system demonstrated the highest and lowest water generation rates under Test 1 and Test 5 conditions, respectively.

Taking Fig. 11 into account, the agreement between the predicted and experimental results was quantitatively evaluated using standard statistical error metrics. The Mean Absolute Percentage Error was calculated as 4.11%, reflecting the high predictive capability of the proposed model. The Root Mean Square Error was obtained as 0.0761, indicating low dispersion between numerical and experimental data. Furthermore, the maximum deviation was determined to be 0.15, observed under Test 4 conditions. These quantitative indicators confirm the robustness and reliability of the developed model.

The average temperature of the heat sink approximates the cold-side average temperature of the thermoelectric module. The average temperatures of the hot-side and cold-side extended temperatures mounted on the hot and cold surfaces of Peltier modules are shown in Fig. 12 for mathematical modeling and experimental study. As expected, during Test 1, high ambient temperature results in high hot-side and cold-side temperatures. On the other hand, during Test 5, the ambient temperature is the lowest at 22.5 ℃, which results in low hot-side and cold-side temperatures. Clearly it is seen that the temperature of both sides is directly affected by the ambient temperature.

Fig. 13 expresses the COP of the Peltier modules during five experimental tests. As it is seen, during Test5, COP is highest. Since COP is defined as the ratio of cooling capacity to electricity consumption and by rising the ambient temperature, the temperature of the cold-side extended surfaces rises and as a result, both cooling capacity and electricity consumption drops which yields higher COP. For the same reason, COP related to Test 5, has the minimum value due to the maximum cooling capacity and maximum electricity consumption by Peltier modules.

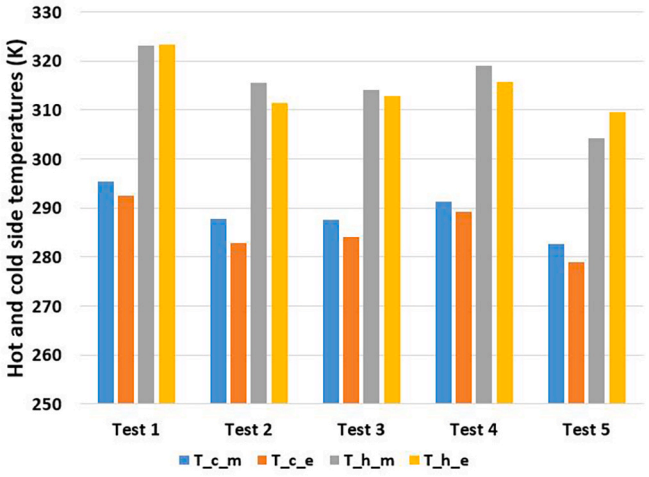

Fig. 12. Temperatures of the hot-side and cold-side extended surfaces.

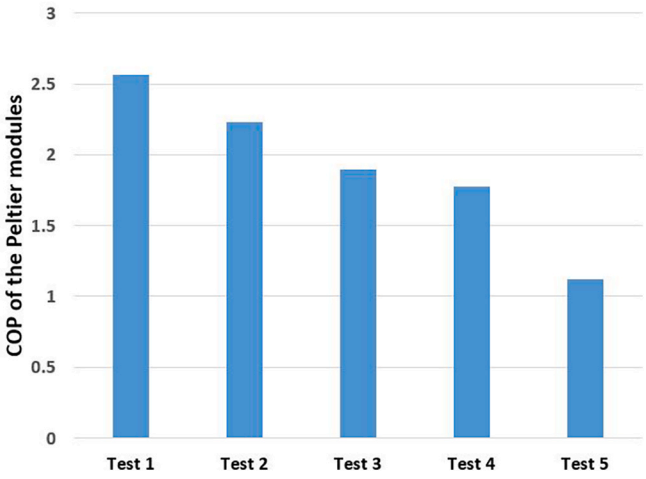

Fig. 13. COP related to Peltier modules during experimental tests.

3.2.2. *Comparison between the effectiveness of the current prototype and remaining Peltier-based AWH systems*

A comparison between the effectiveness of the present prototype and remaining Peltier-based AWH systems reported in literature was performed in this section. The detailed information related to the corresponded studies including ambient temperature, relative humidity, water generation rate and specific power consumption is listed in Table 6. Since, specific energy consumption and water generation rate are playing important role in determining the performance of these systems, these parameters were chosen for comparison. As shown in comparison with the data presented in Table 6, the specific energy consumption of 1.88–2.85 kWh/L demonstrates a favorable performance compared to the values reported in the literature (0.92–12.50 kWh/L), although a direct comparison is limited due to differences in operating conditions. This improvement is likely attributed to the innovative geometry of the inlet and outlet air channels. These channels were designed with a gradually expanding cross-sectional profile, a feature that facilitates smoother airflow induction by the fans toward the

Table 6
Water generation rate and specific energy consumption of the present study with existing literatures.

Prototype	Ambient Temperature (°C)	Relative Humidity (%)	Water Generation Rate (mL/h)	Specific Energy Consumption (kWh/L)
Present study	32	84.8	82.1	2.52
	24.2	85.8	67.9	1.94
	25.4	79	60.4	2.20
	30	78	53.8	2.85
	22.5	69	47.1	1.88
Udomsakdigool et al. [31]	30.5–32	60–75	18.98	1.20
Tan & Fok [32]	29	79	17	7.29
Zhao & Tan [33]	18	60	4	12.50
S. Liu et al. [34]	24.29	67.8	11.2	4.67
Shourideh et al. [30]	3033	6080	3266	1.88
				0.92
Kadhim et al. [35]	31	60	8.1	8.64
	31	65	10.1	6.93
	31	70	16	4.38
	31	75	20	3.50
Casallas et al. [36]	20.6	62.1	2.7	4.63

cold-side extended surfaces. This optimized flow distribution not only enhances air mixing but also improves the overall heat transfer process. Consequently, the system achieves more effective condensation, leading to greater water harvesting efficiency while maintaining reduced energy consumption. This highlights the critical role of geometric optimization in advancing the performance of Peltier-based atmospheric water harvesting systems.

4. Conclusions

This study examines the performance of an atmospheric water collecting system utilizing Peltier modules. The suggested Peltier-cooled AWH system is capable of operating under various humidity levels and may act as an independent system. The research includes mathematical modeling of the system alongside experimental studies. The mathematical modeling of the AWH system evaluates the impact of fin length, ambient air temperature, and ambient relative humidity on COP and daily water production of the system. The experimental tests examine the performance of the system in terms of COP and daily water generation during five test conditions including different ambient temperatures and relative humidity values. The following conclusions have been derived from the present research.

(i) The influence of fin length on daily water production, with water generation peaking at about 2.05 L per day at a length of 0.048 m. Daily water generation rate improves by extending the length of fins until it reaches a maximum, emphasizing the necessity of optimizing these parameters for effective water yield in such systems.

(ii) COP declines with increasing fin length, with a maximum value of 3.43 at a fin length of 0.025 m. This occurs because both energy consumption and cooling capacity increase with extended fin lengths; while electricity consumption increases at a more rapid rate than cooling capacity. This indicates that extended fin lengths are inappropriate from both COP and water generation perspectives.

(iii) Environmental conditions, especially air temperature and relative humidity significantly affects the effectiveness of the Peltier-cooled systems in atmospheric water extraction. Both of these factors are crucial in influencing the water production rate, as they directly impact dehumidification process within these kinds of systems.

(iv) The experimental findings of the Peltier-cooled AWH system reveal that, the present system generates 1.97 L/day during Test 1 (84.8% RH, 32℃), 1.63 L/day during Test 2 (85.8% RH, 24.2℃), 1.45 L/day during Test 3 (79% RH, 25.4℃), 1.29 L/day during Test 4 (76% RH, 30℃) and 1.13 L/day during Test 5 (69 % RH, 22.5 ℃). These results confirm the strong effect of the ambient conditions on the water generation performance of the system.

(v) Results of the heat transfer analysis and experimental study related to hot- and cold-side extended surfaces revealed that the temperature of both sides is directly influenced by the ambient temperature.

(vi) During all five test scenarios, the results of the mathematical model closely match the experimental measurements in terms of daily water generation rates and temperatures of the hot-side and cold-side extended surfaces.

(vii) During Test 1, COP of the Peltier modules reach its maximum due to minimum cooling capacity as well as minimum electricity consumption as the result of highest ambient temperature among all five test conditions. For the same reason, Test 5 yields the minimum COP value due to the maximum cooling capacity and maximum electricity consumption by Peltier modules.

(viii) The predicted results show good agreement with the experimental data for all test cases, with a MAPE of 4.11 %, an RMSE of 0.0761, and a maximum deviation of 0.15, confirming that the proposed model provides accurate and reliable predictions.

(ix) Even though the findings of this study suggest that the suggested Peltier-cooled AWH system is feasible and validated, more research is advised to address some of the system's limitations and improve its applicability. Beyond the current mathematical model, future research should use computational fluid dynamics simulations to further optimize the fin geometry and air flow channels. A crucial step in guaranteeing a completely sustainable, off-grid operation would also be integrating the system with renewable energy sources, like solar photovoltaic panels. Comparing the cost of water production to traditional water supplies requires a thorough economic analysis from the standpoint of commercial viability. A thorough examination of the collected water quality is also necessary to make sure it satisfies potability requirements for human consumption, and long-term durability testing should be carried out to assess the system's dependability over extended periods of time.

CRediT authorship contribution statement

Parisa Heidarnejad: Writing – review & editing, Writing – original draft, Methodology, Conceptualization. **Egemen Sulukan:** Writing – review & editing, Supervision. **Abdullah Dedecan:** Investigation, Data curation. **Ali Kose:** Writing – review & editing, Writing – original draft, Methodology. **Furkan Yildirim:** Writing – review & editing.

Declaration of competing interest

The authors declare that they have no known competing financial interests or personal relationships that could have appeared to influence the work reported in this paper.

Acknowledgment

This work was supported by the Scientific and Technological Research Council of Türkiye (TÜBİTAK) under Project No. 1919B012324368 and İstanbul Gedik University Scientific Research Projects Coordination Unit (BAP) under Project No. GDK202308-26. The Authors also thank the Faculty of Engineering at İstanbul Gedik University for their invaluable support in facilitating this research.

Data availability

Data will be made available on request.

References

[1] D. Seckler, R. Barker, U. Amarasinghe, Water scarcity in the twenty-first century, Int. J. Water Resour. Dev. 15 (1–2) (1999) 29–42, https://doi.org/10.1080/07900629948916.

[2] C. Ingrao, R. Strippoli, G. Lagioia, D. Huisingh, Water scarcity in agriculture: an overview of causes, impacts and approaches for reducing the risks, Heliyon 9 (8) (2023) e18507, https://doi.org/10.1016/J.HELIYON.2023.E18507/ASSET/CBEAB169-04E0-4D7B-8B3A-047B76C12E87/MAIN.ASSETS/GR4.JPG.

[3] M.A. Siddiqui, M.A. Azam, M.M. Khan, S. Iqbal, M.U. Khan, Y. Raffat, Current trends on extraction of water from air: an alternative solution to water supply, Int. J. Environ. Sci. Technol. 20 (1) (2023) 1053–1080, https://doi.org/10.1007/S13762-022-03965-8/METRICS.

[4] H. Lu, W. Shi, Y. Guo, W. Guan, C. Lei, G. Yu, Materials engineering for atmospheric water harvesting: progress and perspectives, Adv. Mater. 34 (12) (2022) 2110079, https://doi.org/10.1002/ADMA.202110079;REQUESTEDJOURNAL:JOURNAL:15214095;WGROUP:STRING:PUBLICATION.

[5] T. Xiang, S. Xie, G. Chen, C. Zhang, Z. Guo, Recent advances in atmospheric water harvesting technology and its development, Mater. Horiz. 12 (4) (2025) 1084–1105, https://doi.org/10.1039/D4MH00986J.

[6] V. Alipour, A.H. Mahvi, L. Rezaei, Quantitative and qualitative characteristics of condensate water of home air-conditioning system in Iran, Desalin. Water Treat. 53 (7) (2015) 1834–1839, https://doi.org/10.1080/19443994.2013.870724.

[7] M. Ejeian, R.Z. Wang, Adsorption-based atmospheric water harvesting, Joule 5 (7) (2021) 1678–1703, https://doi.org/10.1016/J.JOULE.2021.04.005.

[8] B. Tashtoush, A.Y. Alshoubaki, Solar-off-grid atmospheric water harvesting system: performance analysis and evaluation in diverse climate conditions, Sci. Total Environ. 906 (2024) 167804, https://doi.org/10.1016/J.SCITOTENV.2023.167804.
[9] J. Wang, W. Ying, L. Hua, H. Zhang, R. Wang, Global water yield strategy for metal-organic-framework-assisted atmospheric water harvesting, Cell Rep. Phys. Sci. 4 (12) (2023) 101742, https://doi.org/10.1016/j.xcrp.2023.101742.
[10] K. Yang, T. Pan, N. Farhat, A.I. Felix, R.E. Waller, P.Y. Hong, J.S. Vrouwenvelder, Q. Gan, Y. Han, A solar-driven atmospheric water extractor for off-grid freshwater generation and irrigation, Nat. Commun. 15 (1) (2024) 1–9, https://doi.org/10.1038/S41467-024-50715-0.
[11] Z. Zheng, Y. Shi, S. Yan, Q. Yang, Y. Xu, Advances in atmospheric water generation using thermoelectric coolers, Energ. Conver. Manage. 343 (2025) 120193, https://doi.org/10.1016/J.ENCONMAN.2025.120193.
[12] H. Jarimi, R. Powell, S. Riffat, Review of sustainable methods for atmospheric water harvesting, International Journal of Low-Carbon 2020 (2020) 253–276, https://doi.org/10.1093/ijlct/ctz072.
[13] I. Haechler, H. Park, G. Schnoering, T. Gulich, M. Rohner, A. Tripathy, A. Milionis, T.M. Schutzius, D. Poulikakos, Exploiting radiative cooling for uninterrupted 24-hour water harvesting from the atmosphere, Sci. Adv. 7 (26) (2021) 3978–4001, https://doi.org/10.1126/SCIADV.ABF3978/SUPPL_FILE/ABF3978_SM.PDF.
[14] G. Balgurinejad, M. Kalteh, K. Atashkari, H.A. Garmejani, Theoretical assessment of a thermoelectric heat recovery system considering lateral heat rejection and temperature variation of the fluid flow, Therm. Sci. Eng. Prog. 63 (2025) 103692, https://doi.org/10.1016/j.tsep.2025.103692.
[15] X. Zhou, H. Lu, F. Zhao, G. Yu, Atmospheric water harvesting: a review of material and structural designs, ACS Mater. Lett. 2 (7) (2020) 671–684, https://doi.org/10.1021/acsmaterialslett.0c00130.
[16] X. Han, T. Liu, Y. Cai, D. Wang, X. Wei, Y. Hai, R. Shi, W. Guo, Design and evaluation of an innovative thermoelectric-based dehumidifier for greenhouses, Agronomy 15 (5) (2025) 1194, https://doi.org/10.3390/agronomy15051194.
[17] John, J., Ramzan Zafar, H., Francis, J., James, A., Tharian, Dr. M. G., & Mathew, Mr. J. (2022). Design and optimization of an atmospheric water generator using thermoelectric cooling modules. *Materials Today: Proceedings*, *56*, 2563–2567. https://doi.org/10.1016/j.matpr.2021.09.149.
[18] K.H. Lee, O.J. Kim, Analysis on the cooling performance of the thermoelectric micro-cooler, Int. J. Heat Mass Transf. 50 (9–10) (2007) 1982–1992, https://doi.org/10.1016/j.ijheatmasstransfer.2006.09.037.
[19] F. Shahrokhi, A. Esmaeili, Optimizing relative humidity based on the heat transfer terms of the thermoelectric atmospheric water generator (AWG): innovative design, Alex. Eng. J. 67 (2023) 143–152, https://doi.org/10.1016/J.AEJ.2022.09.003.
[20] S. Sanaye, A. Shourabi, D. Borzuei, Sustainable water production with an innovative thermoelectric-based atmospheric water harvesting system, Energy Rep. 10 (2023) 1339–1355, https://doi.org/10.1016/j.egyr.2023.07.062.
[21] D. Milani, A. Abbas, A. Vassallo, M. Chiesa, D.A. Bakri, Evaluation of using thermoelectric coolers in a dehumidification system to generate freshwater from ambient air, Chem. Eng. Sci. 66 (12) (2011) 2491–2501, https://doi.org/10.1016/j.ces.2011.02.018.
[22] A. Alenezi, H.-H. Jung, Y. Alabaiadly, Experimental and numerical analysis of an atmospheric water harvester using a thermoelectric cooler, Atmos. 14 (2) (2023) 276, https://doi.org/10.3390/atmos14020276.
[23] V. Baiju, A. Asif Sha, A.B. Chai, N.F.F. Alhialy, A.G. Nath, A. Sudheer, Performance assessment of a solar hybrid potable atmospheric water generator using vapour adsorption-thermo electric cooling system, Energ. Conver. Manage. 330 (2025) 119665, https://doi.org/10.1016/j.enconman.2025.119665.
[24] H. Xiao, J. Hu, Derivation and verification of the revised thermoelectric energy equations considering convective heat dissipation for engineering calculations and analysis, Therm. Sci. Eng. Prog. 62 (2025) 103654, https://doi.org/10.1016/j.tsep.2025.103654.
[25] K. Irshad, A. Almalawi, K. Habib, M.H. Zahir, A. Ali, S. Islam, B.B. Saha, Experimental study of a thermoelectric air duct dehumidification system for tropical climate, Heat Transfer Eng. 42 (13–14) (2021) 1159–1171, https://doi.org/10.1080/01457632.2020.1777008.
[26] Z. Liu, L. Zhang, G. Gong, Experimental evaluation of a solar thermoelectric cooled ceiling combined with displacement ventilation system, Energ. Conver. Manage. 87 (2014) 559–565, https://doi.org/10.1016/j.enconman.2014.07.051.
[27] Y.A. Çengel, A. J. G. (2011). *Heat and Mass Transfer: Fundamentals & Applications* (McGraw-Hill, Ed.; 4th ed.).
[28] M.A. Muñoz-García, G.P. Moreda, M.P. Raga-Arroyo, O. Marín-González, Water harvesting for young trees using Peltier modules powered by photovoltaic solar energy, Comput. Electron. Agric. 93 (2013) 60–67, https://doi.org/10.1016/j.compag.2013.01.014.
[29] A. Kiliç, K. Onat, The optimum shape for converting rectangular fins when condensation occurs, Wärme- Und Stoffübertragung 15 (2) (1981) 125–133, https://doi.org/10.1007/BF01002408.
[30] A.H. Shourideh, W. Bou Ajram, J. Al Lami, S. Haggag, A. Mansouri, A comprehensive study of an atmospheric water generator using Peltier effect, Therm. Sci. Eng. Prog. 6 (2018) 14–26, https://doi.org/10.1016/j.tsep.2018.02.015.
[31] C. Udomsakdigool, J. Hirunlabh, J. Khedari, B. Zeghmati, Design optimization of a new hot heat sink with a rectangular fin array for thermoelectric dehumidifiers, Heat Transfer Eng. 28 (7) (2007) 645–655, https://doi.org/10.1080/01457630701266470.
[32] F.L. Tan, S.C. Fok, Experimental testing and evaluation of parameters on the extraction of water from air using thermoelectric coolers, J. Test. Eval. 41 (1) (2013) 1–8, https://doi.org/10.1520/JTE20120105.
[33] D. Zhao, G. Tan, A review of thermoelectric cooling: materials, modeling and applications, Appl. Therm. Eng. 66 (1–2) (2014) 15–24, https://doi.org/10.1016/j.applthermaleng.2014.01.074.
[34] S. Liu, W. He, D. Hu, S. Lv, D. Chen, X. Wu, F. Xu, S. Li, Experimental analysis of a portable atmospheric water generator by thermoelectric cooling method, Energy Procedia 142 (2017) 1609–1614, https://doi.org/10.1016/j.egypro.2017.12.538.
[35] T.J. Kadhim, A.K. Abbas, H.J. Kadhim, Experimental study of atmospheric water collection powered by solar energy using the Peltier effect, IOP Conf. Ser.: Mater. Sci. Eng. 671 (1) (2020) 012155, https://doi.org/10.1088/1757-899X/671/1/012155.
[36] I. Casallas, M. Pérez, A. Fajardo, C.-I. Paez-Rueda, Experimental parameter tuning of a portable water generator system based on a thermoelectric cooler, Electronics 10 (2) (2021) 141, https://doi.org/10.3390/electronics10020141.